FACTA UNIVERSITATIS
Series: **Architecture and Civil Engineering** Vol. 2, N° 1, 1999, pp. 41 - 51

STATIC AND DYNAMIC ANALYSIS OF THE ARTA BRIDGE BY FINITE ELEMENTS

UDC 624.21:624.041+042:519.6(045)

G.D. Hatzigeorgiou, D.E. Beskos
D.D. Teodorakopoulos, M. Sfakianakis

Department of Civil Engineering, University of Patras, 26500 Patras, Greece

Abstract. *A finite element methodology is developed for the static and dynamic analysis of large order historical masonry structures and applied to the case of the Arta bridge under plane stress conditions. The inelastic material behavior is simulated with the aid of the theory of continuum damage. The particular theory of damage used is a combination of the Mazars and the Faria and Oliver theories and is characterized by simplicity and successful modeling of the mechanical behavior of masonry structures. In addition, this theory permits the easy calculation of damage indices for the various parts of the structure and the damage index of the whole structure as well. The above finite element method is used to analyze statically and dynamically (seismically) the historic Arta bridge under conditions of plane stress and under both elastic and inelastic material behavior.*

1. INTRODUCTION

The knowledge of the static and/or dynamic response of a historical structure before and after a possible conservation intervention or strengthening is absolutely essential for the determination of its strength and the location of those areas where damage can occur. Basic knowledge on the mechanical behavior of masonry structures can be obtained by studying the excellent book of Tassios (1987).

The determination of the response of complicated geometrically historical masonry structures requires the use of numerical methods of analysis, such as the finite element method. This method is capable of performing static or dynamic analyses of these structures assuming inelastic material behavior (Zienkiewicz and Taylor, 1991). The extensive review article of Beskos (1993-94) on the subject of the use of finite and boundary elements for the analysis of monuments and special structures contains all the relevant bibliography up to 1993. Interesting articles on the topic of the analysis of

Received March 9, 2001

historical structures by analytical or experimental methods can be found in the recent books of Brebbia and Lefteris (1995), Sanchez-Beitia and Brebbia (1997), Rocca et al (1997), Crocci (1998) and Brebbia and Jager (1999).

Elastic analyses of masonry structures can be done very easily by using two- and three- dimensional finite element computer programs, but they do not provide realistic solutions. Reliable solutions are provided by inelastic analyses, which combine the finite element method with a certain model of inelastic behavior of the masonry material.

In general, the existing models of the mechanical behavior of masonry materials can be classified into two large categories, the discrete and the continuum ones, (Beskos, 1993-94). Discrete models are used for the analysis of monumental structures composed of large discrete parts, such as stone arch parts or stone drums of columns of ancient temples. In this case, the discrete elements of the structure are assumed to behave elastically, while the behavior of the contact surface between them is assumed to be described by a unilateral friction law. Continuum models are used for masonry structures composed of a combination of bricks or stones and mortar at their surfaces of contact. The mechanical behavior of the continuum models can be described by a stress-strain law, which is derived from an one-phase or a two-phase model of the masonry material (Beskos, 1993-94).

The one-phase models consider the masonry as consisting of a single material, whose phenomenological behavior is described by an inelastic theory (theory of no-tension, theory of plasticity, theory of damage). Models of this category have been recently used in the framework of the finite element method by, e.g., Oñate et al (1996), Alves and Alves (1997), Lourenco et al (1997), Papa and Nappi (1997) and Genna et al (1998). The two-phase models take into account the different inelastic behavior between the two components of the masonry (brick or stone and mortar) as well as the anisotropy induced by them and on the basis of a homogenization theory result into an inelastic stress-strain law of the masonry material in the framework of the theory of plasticity or damage. Models of this category have been used recently in conjunction with finite elements by, e.g., Swan and Cakmak (1993), Stavrakakis et al (1996), Pegon and Antoine (1997), Luciano and Sacco (1998) and Lopez et al (1999).

The one-phase models are obviously simpler than the two-phase ones and for this reason they can be very successfully used for the analysis of three-dimensional structures of large size and great geometrical complexity. In the present work an one-phase model for masonry structures with different strengths in tension and compression and brittle behavior is employed. This model is created by combining the damage theory of Mazars (1986) and the one by Faria and Oliver (1993). Use of this model in the framework of the finite element method enables us to analyze statically and dynamically (seismically) the historic Arta bridge under plane stress conditions. This bridge has been previously analyzed for its own weight and seismic loading (applying it statically) by Plainis (1992), assuming linear elastic material behavior and plane stress conditions.

2. FORMULATION AND SOLUTION OF THE PROBLEM

Use of the finite element method requires the discretization of the structure into NE finite elements with NN nodes in total. In this work, masonry structures are analyzed under plane stress conditions. Thus, linear isoparametric quadrilateral plane stress elements with four nodes (at their corners) are selected. These elements are better than the corresponding triangular ones because of their higher accuracy and better than the quadratic quadrilateral ones because the latter ones are more computationally expensive, especially for large size problems (Lepi, 1998).

The matrix equation of motion of a structure in the framework of the finite element method has the form (Karabalis and Beskos, 1997)

$$[M]\{\ddot{u}\}+[C]\{\dot{u}\}+\{R\}=\{F\} \tag{1}$$

where [M] and [C] are the mass and damping matrices, respectively, {R} = {R(u)} is the vector of the internal reaction forces (for linear elastic material behavior one has {R}=[K]{u}, where [K] is the stiffness matrix), $\{\ddot{u}\}$, $\{\dot{u}\}$ and $\{u\}$ are the vectors of acceleration, velocity and displacement of the structure, respectively and {F} is the vector of the external loads. The solution of the above equation (1) can be obtained by the employment of a time integration scheme. Here the step-by-step time integration algorithm of Newmark is employed. Thus, the solution of equation (1) requires the application of two groups of steps, where the first group corresponds to the basic computations (Table 1), while the second one is repeated at every time step (Table 2).

Table 1. Application of Newmark's algorithm for non-linear (inelastic) dynamic analysis

PART A

Step 1: Selection of parameters β and γ. The values of β=1/4 and γ=1/2 are selected, which correspond to the case of the average acceleration method.

Step 2: Computation of the initial conditions on the basis of the equation of motion and the use of $\{\dot{u}\}=\{\dot{u}_0\}$ and $\{u\}=\{u_0\}$

Step 3: Selection of the time step Δt.

PART B

Step 1: Computation of the vector of the effective external loads from

$$\{\Delta\hat{R}_{eff}\}=\{\Delta R\}+\left(\frac{4}{\Delta t}[M]\{\ddot{u}^t\}+2[C]\{\dot{u}^t\}\right) \tag{2}$$

Step 2: Computation of the effective stiffness matrix from

$$[\hat{K}_{eff}]=[K^D]+\frac{2}{\Delta t}[C]+\frac{4}{\Delta t^2}[M] \tag{3}$$

where [K^D] is the secant stiffness matrix computed with the aid of the damage d (see section 3) in every finite element.

Step 3: Computation of the vector of the displacement increment with the aid of the modified iteration method of Newton-Raphson (see Table 2).

Step 4: Computation of the vector of the velocity increment of the structural nodes

$$\{\Delta\dot{u}\} = \frac{2}{\Delta t}\{\Delta u\} - 2\{\dot{u}^t\} \tag{4}$$

Step 5: Computation of the vector of the acceleration increment of the structural nodes

$$\{\Delta\ddot{u}\} = \frac{4}{\Delta t^2}\{\Delta u\} - \frac{4}{\Delta t}\{\dot{u}^t\} - 2\{\ddot{u}^t\} \tag{5}$$

Step 6: Computation of the new values of displacements, velocities and accelerations

$$\begin{aligned} \{u^{t+\Delta t}\} &= \{u^t\} + \{\Delta u\} \\ \{\dot{u}^{t+\Delta t}\} &= \{\dot{u}^t\} + \{\Delta\dot{u}\} \\ \{\ddot{u}^{t+\Delta t}\} &= \{\ddot{u}^t\} + \{\Delta\ddot{u}\} \end{aligned} \tag{6}$$

Table 2. Modified iteration method of Newton-Raphson

Step 1: Initial values are assumed for the vectors $\{u_{(0)}^{t+\Delta t}\}, \{F_{(0)}\}, \{\Delta R_{(1)}\}$

Step 2: The following vectors are computed repeatedly until convergence occurs

$$\begin{aligned} &[K^D]\{\Delta u_{(k)}\} = \{\Delta R_{(k)}\} \Rightarrow \{\Delta u_{(k)}\} = [K^D]^{-1}\{\Delta R_{(k)}\} \\ &\{u_{(k+1)}^{t+\Delta t}\} = \{u_{(k)}^{t+\Delta t}\} + \{\Delta u_{(k)}\} \\ &\{\Delta Q_{(k)}\} = \{F_{(k)}\} - \{F_{(k-1)}\} + ([\hat{K}_{eff}] - [K^D])\{\Delta u_{(k)}\} \\ &\{\Delta R_{(k+1)}\} = \{\Delta R_{(k)}\} - \{\Delta Q_{(k)}\} \end{aligned} \tag{7}$$

3. DETERMINATION OF DAMAGE

The stiffness matrix of inelastic structures is not constant but varies as the loading on the structure varies. Thus, in the framework of the finite element method, the secant stiffness matrix is evaluated on the basis of the value of the damage at every Gauss point of every element and at every time step. That value of the damage is determined by using the damage evolution law provided by the damage theory employed. In this work use is made of the FOM damage model. This is a combination between the elastic-damage part of the elastoplastic-damage model of Faria and Oliver (1993) with two damage indices (one for compression and one for tension) and the damage theory of Mazars (1986), which unifies appropriately these two indices into one index.

With the above FOM damage model, all the basic characteristics of the mechanical behavior of brittle type of materials like masonry, i.e., the different behavior in tension and compression, the reduction of stiffness and strength with deformation, the localization of deformation and the mesh independent character of the FEM solution are taken into account. The FOM model, in addition to its relative simplicity with respect to other damage models, is capable of taking into account the strength increase under biaxial or triaxial stress states observed in experiments. The application of the FOM model requires the execution of the five steps of Table 3.

Table 3. Computational procedure for the FOM damage model

Step 1: Computation of the effective strains $<\varepsilon_i>$ and $>\varepsilon_i<$ from the principal strains $\{\varepsilon_i\}$ where i = 1,2,3 and $\{\varepsilon\}=[B]\{u\}$

$$\begin{array}{lclcl} <\varepsilon_i>=\varepsilon_i & & >\varepsilon_i<=0 & & \varepsilon_i>0 \\ & \text{and} & & \text{when} & \\ <\varepsilon_i>=0 & & >\varepsilon_i<=\varepsilon_i & & \varepsilon_i\le 0 \end{array} \tag{8}$$

and the equivalent strains in tension and compression

$$\tilde{\varepsilon}^+ = \sqrt{\sum_{i=1}^{2} <\varepsilon_i>^2} \quad \text{and} \quad \tilde{\varepsilon}^- = \sqrt{\sum_{i=1}^{2} >\varepsilon_i<^2} \tag{9}$$

from the effective ones

Step 2: Computation of the effective true stresses $<\bar{\sigma}_i>$ and $>\bar{\sigma}_i<$ from the true principal stresses $\{\bar{\sigma}_i\}$ which are obtained from $\{\bar{\sigma}\}=[D]\{\varepsilon\}$

$$\begin{array}{lclcl} <\bar{\sigma}_i>=\bar{\sigma}_i & & >\bar{\sigma}_i<=0 & & \bar{\sigma}_i>0 \\ & \text{and} & & \text{when} & \\ <\bar{\sigma}_i>=0 & & >\bar{\sigma}_i<=\bar{\sigma}_i & & \bar{\sigma}_i\le 0 \end{array} \tag{10}$$

and the equivalent stresses in tension and compression from the effective ones

$$\bar{\sigma}^- = \sum_{i=1}^{3} >\bar{\sigma}_i< \quad \text{and} \quad \tilde{\sigma}^- = \sqrt{\sum_{i=1}^{3} (>\bar{\sigma}_i<)^2} \tag{11}$$

Use of Hooke's law to compute the strains in tension and compression from the effective true stresses

$$\{\bar{\varepsilon}^+\} = [D]^{-1}\{<\bar{\sigma}_i>\} \quad \text{and} \quad \{\bar{\varepsilon}^-\} = [D]^{-1}\{>\bar{\sigma}_i<\} \tag{12}$$

Step 3: Determination of the parameters α^+ and α^- of the deformation

$$\alpha^+ = \frac{2k^+ + k^-}{2k^+} \quad \text{and} \quad \alpha^- = \frac{k^+ + k^-}{k^-} \tag{13}$$

where

$$k^+ = \sum_{i=1}^{3} H_i^+ \frac{\bar{\varepsilon}_i^+(\bar{\varepsilon}_i^+ + \bar{\varepsilon}_i^-)}{(\tilde{\varepsilon}^+)^2} \quad \text{and} \quad k^- = \sum_{i=1}^{3} H_i^- \frac{\bar{\varepsilon}_i^-(\bar{\varepsilon}_i^+ + \bar{\varepsilon}_i^-)}{(\tilde{\varepsilon}^-)^2} \tag{14}$$

with

$$\begin{array}{lclcl} H_i^+ = 1 & & H_i^+ = 1 & & (\bar{\varepsilon}_i^+ + \bar{\varepsilon}_i^-) < 0 \\ & \text{and} & & \text{for} & \\ H_i^+ = 0 & & H_i^+ = 0 & & (\bar{\varepsilon}_i^+ + \bar{\varepsilon}_i^-) \ge 0 \end{array} \tag{15}$$

Step 4: Computation of the equivalent effective tensile and compressive stress (see Step 2)

$$\bar{\tau}^+ = \sqrt{\{<\bar{\sigma}>\}^T [D^{-1}] \{<\bar{\sigma}>\}} \tag{16}$$

and

$$\bar{\tau}^- = \sqrt{\sqrt{3}(K\bar{\sigma}_{oct}^- + \bar{\tau}_{oct}^-)} \tag{17}$$

where K is a material constant given by

$$K = \sqrt{2}\,\frac{1-R_0}{1-2R_0} \quad \text{with} \quad R_0 = \frac{f_{0-2D}^-}{f_{0-1D}^-} \tag{18}$$

and the octahedral stresses are given by

$$\bar{\sigma}_{oct}^{-} = \frac{\bar{\sigma}^{-}}{3} \quad \text{and} \quad \bar{\tau}_{oct}^{-} = \frac{1}{3}\sqrt{3(\tilde{\sigma}^{-})^{2} - (\bar{\sigma}^{-})^{2}} \tag{19}$$

Step 5: Computation of the evolution of the damage indices d^{+} and d^{-} during the deformation from

$$d^{+} = 1 - \frac{r_0^{+}}{\tau^{+}} e^{A^{+}\left(1 - \frac{\tau^{+}}{r_0^{+}}\right)} \quad \text{and} \quad d^{-} = 1 - \frac{r_0^{-}}{\tau^{-}}(1 - A^{-}) - A^{-} e^{B^{-}\left(1 - \frac{\tau^{-}}{r_0^{-}}\right)} \tag{20}$$

where

$$r_0^{+} = \frac{f_t}{\sqrt{E}} \quad \text{and} \quad r_0^{-} = \sqrt{\sqrt{\frac{2}{3}} \frac{R_0}{1 - 2R_0} f_c} \tag{21}$$

and A^{+}, A^{-} and B^{-} are parameters determining the descenting branch of the stress-strain diagram. These parameters depend on the tensile f_t and compressive f_c strength, the fracture energy G_f and the internal length scale l^{*}. A detailed determination of them is described by Faria & Oliver (1993). The total damage index d is finally computed with the aid of relations (13) and (20) as

$$d = \alpha^{+} d^{+} + \alpha^{-} d^{-} \tag{22}$$

The tensor of the total stresses is then computed as

$$\{\sigma\} = (1 - d)\{\bar{\sigma}\} = (1 - d)[D]\{\varepsilon\} \tag{23}$$

Relation 23 is used to determine the secant stiffness matrix at every time step. The total one-dimensional stress-strain curve and the bounding damage surface in the two-dimensional stress space for the FOM model are shown in Figure 1.

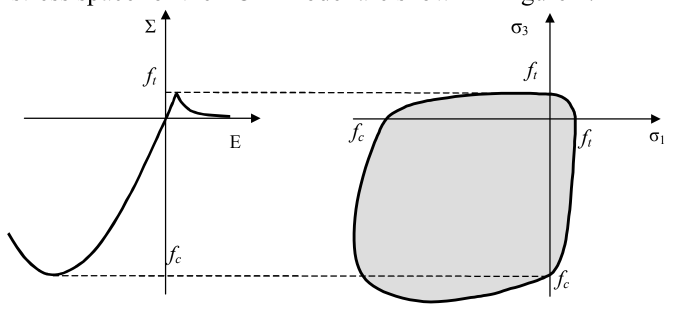

Fig. 1. The bounding surface of damage model FOM

4. ANALYSIS OF THE ARTA BRIDGE

4.1. Introductory remarks about the bridge

The Arta bridge is built in the city of Arta, Epirus, Greece over the river Arachthos. It appears that the bridge was erected during the 13th century A.D., even though there is historical evidence indicating that a bridge had been built in the same location during the classical or the Hellenistic period. This bridge is well known all over Greece because of the difficulty its builders had in erecting it, a fact that led to the composition of a popular song, which is still sang in Greece even to this day. Since 1960 the bridge is used exclusively as a pedestrian bridge. A few years ago the bridge was reinforced and retrofitted and serves as a tourist attraction for the city of Arta.

The structure consists of four main arches with spans of 23.95 m, 15.83 m, 15.43 m and 16.16 m, while there are various relief openings above the piers. The width of the superstructure of the bridge at the top is 3.70 m, while the net width of the road is equal to 3.00 m. The material parameters of the bridge have been determined to have the following values: modulus of elasticity $E = 3.0$ GPa, Poisson's ratio $\nu = 0.22$, uniaxial compressive strength $f_c = 30.0$ MPa, biaxial compressive strength $f_{C2D} = 34.8$ MPa and mass density $\rho = 2700$ kg/m^3. Three different values of uniaxial tensile strength ($f_t = 0.30$, 0.40 and 0.50 MPa) and fracture energy ($G_f = 20$, 40 and 60 N/m) are examined (cases I, II and III, respectively). The finite element mesh used to discretize the bridge is shown in Figure 2.

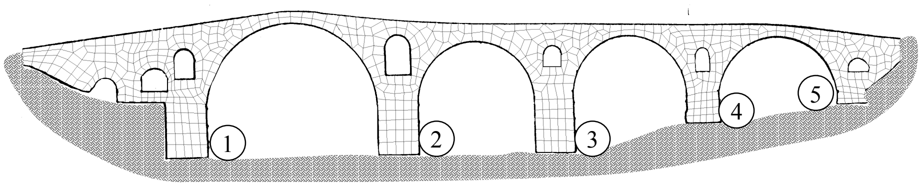

Fig. 2. Discretization of the structure

4.2. Elastic and inelastic static analysis

The structure is initially loaded statically by its own weight and the analysis shows nowhere any damage. Subsequently, the structure loaded by its own weight is additionally subjected to a ground settlement δ at the support of pier number 2. With an increase of the support yielding, a state of stress is created, which leads to damage, mainly at the ends of the arches on either side of the yielded support, as shown in Figure 3 for the case of $f_t = 0.5$ MPa, $G_f = 60.0$ N/m and $\delta = 50$ mm. The observed local damage is due to the development of tensile stresses there in excess of the tensile strength of the masonry. Thus, increase of the tensile strength there, e.g., by reinforcing steel bars, can lead to a decrease of the damage in both local and global level.

The total damage index D for the whole structure can be obtained in terms of the local damage index d at every point of the total volume Ω of the structure in accordance with the suggestion of Cervera et al (1995) as

$$D = \sqrt{\int_\Omega (d)^2 d\Omega \Big/ \int_\Omega d\Omega} \tag{24}$$

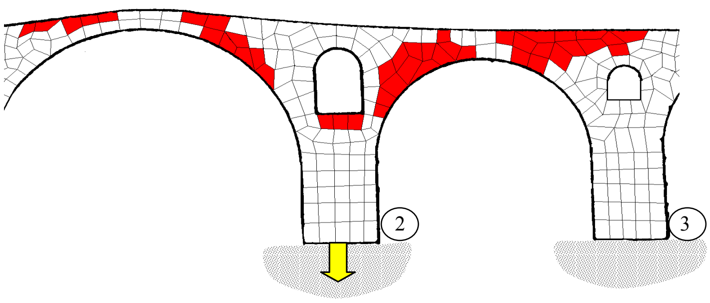

Fig. 3. Damaged region of the structure with settlement $\delta = 50$ mm

Figure 4 depicts the global damage index D for various values of the settlement δ for the three cases I, II and III.

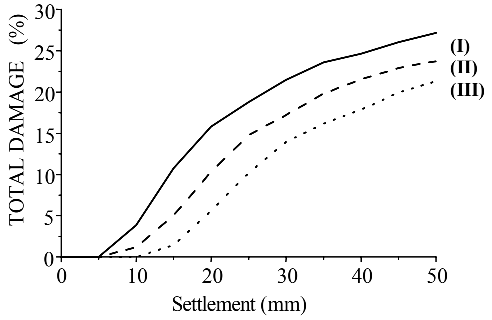

Fig. 4. Total damage-settlement diagram of the structure

4.3. Elastic and inelastic dynamic analysis

The bridge is now assumed to be subjected to a seismic excitation described by the first 5 secs of the N-S component of the El Centro 1940 earthquake and depicted in Figure 5 in the form of an acceleration versus time curve.

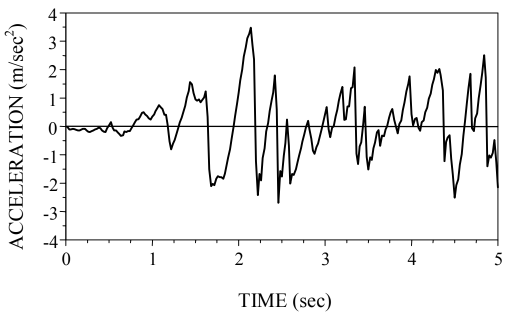

Fig. 5. Ground acceleration of ElCentro (1940) earthquake (N-S direction)

The above accelerogram acts on the structure along the horizontal direction of the bridge (the same at all the pier bases simultaneously), while the same accelerogram multiplied by the reduction factor 2/3 acts along the vertical direction of the bridge (the same at all the pier bases simultaneously).

According to the Greek seismic code N.E.A.K. (1995) the maximum expected ground acceleration in the Arta region is equal to 16% of the gravity acceleration, while the El Centro accelerogram of Figure 5 shows a maximum ground acceleration of 34%. Hence the El Centro accelerogram is multiplied by the reduction factor 0.47 (= 0.16/0.34) for the horizontal and by 0.31 (= [0.16/0.34] $\times$ 2/3) for the vertical component of the applied to the bridge seismic excitation. The bridge was analyzed by assuming elastic and inelastic material behavior with f_t = 0.3 MPa and G_f = 20 N/m (case I). Figure 6 shows the time history of the horizontal displacement of the top of pier number 2 of the bridge for the elastic and inelastic case and for the load combination “self-weight + earthquake”. Figure 7 provides a picture of the damage distribution in the bridge for the above load combination and indicates that the damage concentrates at the upper part of the bridge, while the piers show no damage.

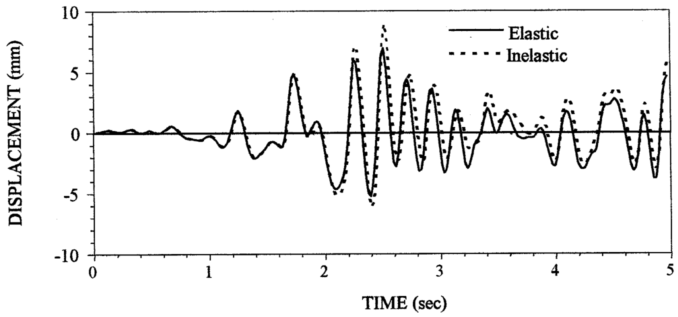

Fig. 6 . Horizontal displacement time history

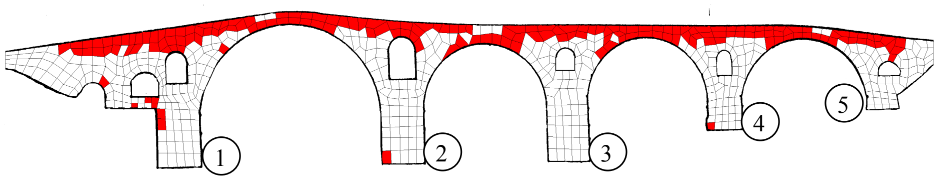

Fig. 7. Damaged region of the structure: 'self weight + earthquake' load combination

5. CONCLUSIONS

In the present work a finite element method of analysis of historical masonry structures exhibiting linear elastic or inelastic material behavior under static or dynamic loading was presented. The inelastic behavior is successfully simulated in an efficient manner by a continuum damage theory for brittle materials. This method was used to analyze the response of the historic Arta bridge under plane stress conditions to static and seismic loads. For this structure and for the various loading cases, the local and global damage indices were determined. From the various analyses one can conclude that the probable ground settlements at one or more pier supports and the seismic excitation stress the bridge considerably creating damage at critical areas. On the contrary, the bridge response to self-weight is purely elastic with nowhere any damage. Finally, one can also observe that the inelastic material modeling is essential for a realistic determination of the bridge response and the critical and hence sensitive areas of the structure to the various loading conditions.

REFERENCES

1. Alves, M.K. & Alves, B.K., (1997), *No-tension elastic materials*, Eur. J. Mech., A/Solids, Vol. 16, pp. 103-116.
2. Beskos, D.E. (1993-94), *Use of finite and boundary elements for the analysis of monuments and special buildings*, Bull. Greek Soc. Civil Engrs, Athens, 1993 No 216, pp. 31-43 & 1994, No 217, pp. 15-32.
3. Brebbia, C.A. and Jager, W. (eds.) (1999), *Structural Studies, Repairs and Maintenance of Historical Buildings VI*, Computational Mechanics, Southampton.
4. Brebbia, C.A. and Lefteris, B. (eds.) (1995), *Structural Studies of Historical Buildings IV*, 2 vols, Computational Mechanics Publications, Southampton.
5. Cervera, M., Oliver, J. & Faria, R., (1995), *Seismic evaluation of concrete dams via continuum damage models*, Earth. Engng. Struct. Dyn., Vol. 24, pp. 1225-1245.
6. Croci, G. (1998), *The Conservation and Structural Restoration of Architectural Heritage*, Computational Mechanics Publications, Southampton.
7. Faria, R, & Oliver, X., (1993), *A rate dependent plastic-damage constitutive model for large-scale computations in concrete structures*, Monografia No 17, CIMNI, Spain,.
8. Genna, F., Di Pascua, M. Veroli, M. & Ronca, P., (1998), *Numerical analysis of old masonry buildings: a comparison among constitutive models*, Engng Struct., Vol. 20, pp.37-53.
9. Karabalis, D.L. & Beskos, D.E., (1997), *Numerical methods in earthquake engineering, in Computer Analysis and Design of Earthquake Resistant Structures*, Beskos, D.E. and Anagnostopoulos, S.A (eds.), Computational Mechanics Publications, Southampton, pp.1-102.
10. Lepi, S.M., (1998), *Practical Guide to Finite Elements: a Solid Mechanics Approach*, Marcel Dekker Inc., U.S.A.
11. Lopez, J., Oller, S., Oñate, E. & Lubliner, J., (1999), *A homogeneous constitutive model for masonry*, Int. J. Num. Meth. Engng, Vol. 46, pp. 1651-1671.
12. Lourenco, P.B., de Borst, R., & Rots, J.G., (1997), *A plane stress softening plasticity model for orthotropic materials*, Int. J. Num. Meth. Engng, Vol. 40, pp. 4033-4057.
13. Luciano, R. & Sacco, E., (1998), *A damage model for masonry structures*, Eur. J. Mech., A/Solids, Vol. 17, pp. 285-303.
14. Mazars, J., (1986), *A description of micro- and macroscale damage on concrete structures*, Engng. Fracture Mech., Vol. 25, 5-6, pp. 729-737.
15. *NEAK-New Greek Aseismic Code* (1995), Aseismic Planning and Protection Organization of Greece, Athens.
16. Oñate, E., Hanganu, A., Barbat, A., Oller, S., Vitaliani, R., Saetta, A. & Scotta, R., (1996), *Structural analysis and durability assessment of historical constructions using a finite element damage model*, Publication CIMNE No 73, Barcelona, Spain.
17. Papa, E. & Nappi, A. (1997), *Numerical modeling of masonry: a material model accounting for damage effects and plastic strains*, Appl. Math. Modelling, Vol. 21, pp. 319-335.
18. Pegon, P. & Anthoine, A., (1997), *Numerical strategies for solving continuum damage problems with softening: application to the homogenization of masonry*, Comp. Struct., Vol. 64, pp. 623-642.
19. Plainis, P., (1992), *Arta Bridge: investigations and study of structural behaviour*, CEEC - Civil Engineering European Courses, Mechanics and Structural Restoration of Masonry Structures, Athens.
20. Roca, P. Conzalez, J.L., Mari, A.R. & Oñate, E. (eds.), (1997), *Structural Analysis of Historical Constructions: Possibilities of Numerical and Experimental Techniques*, CIMNE, Barcelona, Spain.
21. Sanchez-Beitia, S. and Brebbia, C.A. (eds.) (1997), *Structural Studies, Repairs and Maintenance of Historical Buildings V*, Computational Mechanics, Southampton.
22. Stavrakakis, E.J., Ignatakis, C.E., Samuel, A.G. & Penelis, G.G., (1996), *Behaviour of masonry under concentrated loading: analytical parametric investigation using the F.E. Method*, in Proc. 2nd Nat. Congress on Computational Mechanics, Sotiropoulos, D.A. & Beskos, D.E. (eds.), Technical University of Crete, Chania, pp. 204-211.
23. Swan, C.C., & Cakmak, A.S., (1993), *Nonlinear quasistatic and seismic analysis of the Agia Sophia using an effective medium approach*, Soil Dyn. Earthq. Engng, Vol. 12, pp. 259-271.
24. Tassios, T.P. (1987), *The Mechanics of Masonry*, Symmetria Publishing, Athens.
25. Zienkiewicz, O. C. and Taylor, R. L., (1991), *The Finite Element Method*, Vol. 1-2, 4th ed., Mc Graw Hill, London.

ANALIZA MOSTA ARTA NA STATIČKA I DINAMIČKA DEJSTVA PRIMENOM METODE KONAČNIH ELEMENATA

G.D. Hatzigeorgiou, D.E. Beskos, D.D. Teodorakopoulos, M. Sfakianakis

Metoda konačnih elemenata je razvijena i za statičku i dinamičku analizu velikih konstrukcija drevnog zidarstva i primenjena je u slučaju mosta Arta pod uslovima ravanskog stanja napona. Neelastično ponašanje materijala se simulira uz pomoć teorije oštećenja kontinuma. Posebna teorija oštećenja koja je korišćena u kombinaciji sa teorijama Mazara, Farie i Olivera i koja je karakteristična jednostavnošću i uspešnim modelovenjem mehaničkog ponašanja zidanih konstrukcija. Uz to, ova teorija omogućava lako izračunavanje indeksa oštećenja za različite delove konstrukcije kao i indeks štete cele konstrukcije. Pomenuta metoda konačnih elemenata je korišćena da se izvrši analiza statističkih i dinamičkih tj. seizmičkih dejstava na istorijskom mostu Arta pod uslovima ravanskog stanja napona pri elastičnom i neelastičnom ponašanju materijala.